EUROPEAN RESPIRATORY *journal*

FLAGSHIP SCIENTIFIC JOURNAL OF ERS

Early View

Original article

Nanoparticle diffusion in spontaneously expectorated sputum as a biophysical tool to probe disease severity in COPD

Jane F. Chisholm, Siddharth K. Shenoy, Julie K. Shade, Victor Kim, Nirupama Putcha, Kathryn A. Carson, Robert Wise, Nadia N. Hansel, Justin S. Hanes, Jung Soo Suk, Enid Neptune

Please cite this article as: Chisholm JF, Shenoy SK, Shade JK, *et al*. Nanoparticle diffusion in spontaneously expectorated sputum as a biophysical tool to probe disease severity in COPD. *Eur Respir J* 2019; in press (https://doi.org/10.1183/13993003.00088-2019).

Nanoparticle diffusion in spontaneously expectorated sputum as a biophysical tool to probe disease severity in COPD

Jane F. Chisholm[1,2], Siddharth K. Shenoy[1,7], Julie K. Shade[1,3], Victor Kim[4], Nirupama Putcha[5], Kathryn A. Carson[6], Robert Wise[5], Nadia N. Hansel[5], Justin S. Hanes[1-3,7†], Jung Soo Suk[1,7†], and Enid Neptune[5†]

[1]Center for Nanomedicine, Wilmer Eye Institute, Johns Hopkins University School of Medicine, Baltimore, MD 21231

[2]Department of Chemical & Biomolecular Engineering, Johns Hopkins University, Baltimore, MD 21218

[3]Department of Biomedical Engineering, Johns Hopkins University, Baltimore, MD 21205

[4]Department of Thoracic Medicine and Surgery, Temple University School of Medicine, Philadelphia, PA 19140

[5]Division of Pulmonary and Critical Care Medicine, Johns Hopkins University School of Medicine, Baltimore, MD 21205

[6]Department of Epidemiology, Johns Hopkins University School of Medicine, Baltimore, MD 21205

[7]Department of Ophthalmology, Wilmer Eye Institute, Johns Hopkins University School of Medicine, Baltimore, MD 21231

† indicates equal contribution and to whom correspondence should be addressed

Enid Neptune eneptune@jhmi.edu

Jung Soo Suk jsuk@jhmi.edu

Justin Hanes hanes@jhmi.edu

Abstract

Rationale: Perturbations in airway mucus properties contribute to lung function decline in patients with chronic obstructive pulmonary disease (COPD). While alterations in bulk mucus rheology have been widely explored, microscopic mucus properties that directly impact on dynamics of microorganisms and immune cells in the COPD lungs are yet to be investigated.

Objectives: We hypothesized that a tightened mesh structure of spontaneously expectorated mucus (i.e. sputum) would contribute to COPD disease severity. Here, we investigated whether the mesh size of COPD sputum, quantified by muco-inert nanoparticle (MIP) diffusion, correlated with sputum composition and lung function measurements.

Methods: The microstructure of COPD sputum was assessed based on the mean-squared displacement (MSD) of variously sized MIP measured by multiple particle tracking. MSD values were correlated with sputum composition and spirometry. Thirty-three samples collected from COPD or non-COPD individuals were analyzed.

Results: We found that 100 nm MIP differentiated microstructural features of COPD sputum. The mobility of MIP was more hindered in sputum samples from severe COPD patients, suggesting tighter mucus mesh size. Specifically, MSD values inversely correlated with lung function.

Conclusions: These findings suggest that sputum microstructure may serve as a novel risk factor for COPD progression and severity.

Word count for abstract: 196

Key Words: COPD sputum, multiple particle tracking, mucus-penetrating particles, muco-inert nanoparticles

Introduction

Mucus abnormalities contribute to chronic morbidity in a variety of lung diseases, including chronic obstructive pulmonary disease (COPD) [1, 2], cystic fibrosis (CF) [3], and asthma [4]. COPD is the third leading cause of death in the US [5], and at least 30% of people with COPD have chronic bronchitis (CB), characterized by chronic cough and sputum production [6, 7]. In healthy lungs, mucus that lines the luminal surface of lung airways serves a critical protective purpose by trapping inhaled particulates and pathogens that are subsequently cleared from the airways via mucociliary clearance (MCC) [8-10]. However, in obstructive lung diseases, mucus hypersecretion can overwhelm MCC and results in bacterial overgrowth, chronic airway inflammation, and airway obstruction [11]. Specifically in COPD, mucus hypersecretion is associated with accelerated lung function decline [12], increased hospitalization rate, and increased mortality [13]. Mucus obstruction of the small airways is also a significant predictive factor of COPD progression and mortality [14, 15], as well as exacerbation risk [16-18].

Airway mucus is a viscoelastic gel comprised of a complex mixture of high molecular weight mucin glycoproteins, cells, cellular debris, bacterial proteins, antibacterial products, and other molecules [19]. Alterations in the composition of mucus directly affect its biophysical properties, resulting in suboptimal MCC and subsequent disease manifestations [20]. In COPD patients with CB, an enhanced expression of gel-forming mucins and elevated overall sputum solids content is observed in the lumen of the small airways [21, 22]. Recently, Anderson and colleagues found that increased solids content in sputum samples from CB patients correlated with elevated partial osmotic pressure of the mucus gel layer and impaired mucus clearance [23]. Functional MCC is dependent on appropriate rheological properties of airway mucus [24]. Macro- (or bulk-) rheological measurements have revealed an increased viscoelasticity of COPD sputum compared to samples from healthy subjects [25]. However, conventional bulk rheology measurements do not reveal properties of mucus or sputum at the microscopic level

which significantly contributes to mucus physiology and may correlate with disease pathology [26].

The diffusion rate of variously-sized nanoparticles has been employed as a biophysical tool to probe the microstructure of airway secretions [27-29], as well as other biological specimens, including the vitreous gel [30], brain extracellular matrix [31] and tumor tissues [32]. Compared to other methods such as fluorescence recovery after photobleaching (FRAP), multiple particle tracking (MPT) allows simultaneous tracking of hundreds of individual particles in highly complex and heterogeneous biological specimens at high spatiotemporal resolution and quantification of individual particle transport rates [33]. We have previously shown that densely coating nanoparticle surfaces with polyethylene glycol (PEG) produces muco-inert nanoparticles (MIP), also known as mucus-penetrating particles (MPP), that are capable of moving in human mucus secretions without being trapped by adhesive interactions [27-29, 34]. The diffusion of MIP in mucus is thus primarily slowed by steric interaction imposed by the microstructure of the gel. In other words, MIP of a given size will move more slowly in a mucus sample with a tighter mesh, especially if the MIP diameter approaches the average pore size of the mucus [27-29]. Conversely, conventional polymeric nanoparticles are trapped in mucus regardless of particle size due to adhesive interactions with mucus constituents; such particles are referred to as conventional particles or muco-adhesive particles (MAP). In this study, we characterized MIP diffusion in spontaneously expectorated sputum from a cohort of cigarette smokers with and without airway obstruction to assess whether the sputum microstructure that governs MIP transport is associated with COPD disease severity and airway obstruction**.**

Methods

MIP were prepared and characterized as previously described [28]. MPT was used to measure mean squared displacement (MSD) of fluorescently labeled MIP and MAP in freshly expectorated sputum samples from non-COPD smokers and COPD patients [33]. The percent solids content of sputum was determined by weighing a given sample followed by freeze-drying and re-weighing the same sample. The concentrations of mucin and DNA in individual sputum samples were measured by fluorometric assays as previously described [28]. Statistical analyses were conducted using Wilcoxon signed rank test for paired comparisons, Wilcoxon rank sum test for two-sample comparisons, and one-way analysis of variance (ANOVA) or Kruskal-Wallis test for comparing more than two groups. Detailed experimental procedures are provided in the Supplementary Material.

Results

Participant characteristics

Demographic data was available on 33 participants: 7 smokers, 18 with mild-moderate COPD (mCOPD), and 8 with moderate-severe COPD (sCOPD) (Table 1). The transport analysis was conducted with sputum samples from 32 participants. Correlations between microstructure, biochemical composition and lung function parameters were also applied to all 33 participants (including one participant's sample without MPT analysis).

Transport of nanoparticles in spontaneously expectorated sputum from smokers without airway obstruction

Nanoparticle movement in mucus approximates both the mesh “tightness” and the pore size within the mucus gel [28]. To establish whether differences in particle diameter and mucus adhesivity affected particle movement in sputum from non-COPD smokers, we first compared the transport behaviors of MIP to those of similarly sized MAP in spontaneously expectorated sputum samples from smokers without airway obstruction (N = 7). The dense PEG coating on the MIP resulted in a slightly increased particle diameter and near neutral surface charge as measured by the ζ-potential (Table 2). For simplicity, we refer to nanoparticles based on their nominal sizes as reported in Table 2. We also confirmed that, unlike MAP, the muco-inert PEG coating effectively precluded adsorption of mucins on the surface of MIP, confirming their muco-resistance (Figure S1). We found that diffusion of MAP, regardless of particle diameter, were largely hindered in sputum samples, as evidenced by the highly confined trajectories (Figure 1A, MAP). In contrast, 100 nm MIP rapidly moved through the sputum sample (Movie E1), as evidenced by their diffusive trajectories (Figure 1A). We further quantified diffusion rates of each particle type, as determined by mean squared displacement (MSD). The MSD represents a square of distance traveled by individual particles at a given time interval (i.e. time scale or τ); thus, MSD is directly proportional to particle diffusion rate. Of note, we compared MSD values among different test groups at τ = 1 s throughout the study, given the limited effects of both static and dynamic errors in particle tracking analysis at τ = 1 s [33]. We found that 100 nm particles displayed a statistically significant difference in MSD between the MIP and MAP at τ = 1 s (Figure 1B; $p < 0.05$); in contrast, the differences were not significant for 300 and 500 nm particles (Figure 1C & D). The tracking resolution was determined to be $\log_{10}(MSD_{\tau=1s})$ of -3 based on the MSD values of particles immobilized in glue.

Transport of nanoparticles in spontaneously expectorated sputum from patients with COPD

We next compared the diffusion of MAP and MIP in sputum samples collected from patients with COPD (N ≥ 13). Unlike 100 nm MAP that showed highly confined trajectories, we found that the similarly sized MIP were capable of diffusing in sputum samples relatively unhindered (100 nm MIP; Figure 2A). The MSD values were significantly greater for MIP in comparison to MAP (Figure 2B). Similar to the observation with sputum samples from non-COPD smokers, both MAP and MIP possessing particle diameters ≥ 300 nm exhibited confined or highly hindered trajectories in COPD sputum samples (Movie E3 for 500 nm MIP). We also found that both 300 and 500 nm MIP exhibited highly restricted motions in sputum samples. However, MSD values were significantly greater for 300 and 500 nm MIP in comparison to the respective MAP (Figure 2B, $p < 0.05$), presumably due to the larger sample size compared to the studies with non-COPD smoker samples.

Transport of individual MIP in sputum samples from smokers without airway obstruction, with mild-moderate COPD, and with severe COPD

We next analyzed MSD values of individual MIP with different particle sizes in sputum samples from non-COPD smokers and COPD patients. The diffusion rates of 100 nm MIP, as measured by MSD, appeared to decrease with the increase in disease severity (Smoker > mCOPD > sCOPD; Figure 3A). The difference was more pronounced when comparing two extreme conditions of Smoker versus sCOPD, as evidenced by the clear leftward shift of the MSD distribution (i.e. greater fractions of MIP with lower MSD values). In general, similar trends were observed with 300 and 500 nm MIP where the fractions of rapidly moving particles (i.e. particles with high MSD values) tended to decrease with respect to disease severity (Figures 3B, C). However, 300 nm MIP exhibited similar overall MSD distributions, as well as median MSD values, in sputum samples from non-COPD smokers and mCOPD patients, while the

distribution in sCOPD samples was clearly leftward-shifted (Figure 3B). As expected from the larger particle diameters, the median MSD values of 500 nm MIP were smaller than those of 100 and 300 nm MIP by about an order of magnitude or more regardless of disease severity (Figure 3C). In particular, the MSD values of a large fraction of 500 nm MIP were below the tracking resolution ($\log_{10}(MSD_{\tau=1s}) < -3$) or approaching it in sCOPD samples, which suggests that 500 nm MIP are significantly larger than the sputum average pore size. We found that median MSD values, specifically $\log_{10}$(median $MSD_{\tau=1s}$), of 100 nm MIP were able to distinguish disease severity, yielding a statistical significant difference between Smoker and sCOPD groups (Figure S2A). However, $\log_{10}$(median $MSD_{\tau=1s}$) of larger MIP were unable to do so (Figures S2B, C). Of note, median MSD values of 100 nm MIP were at least an order of magnitude greater than the tracking resolution regardless of disease severity, providing confidence of our measurement. We then confirmed that size-corrected median MSD values within each disease severity group did not exhibit statistically significant differences, suggesting that all probe particles experienced a similar microstructure regardless of particle size (Figure S3).

In parallel, we conducted an identical analysis with differently sized MAP. While MSD distributions of 100 nm MAP exhibited weaker but similar general trends as those of 100 nm MIP (Figure S4), disease severity could not be differentiated by the $\log_{10}$(median $MSD_{\tau=1s}$) of 100 nm MAP (Figure S5A) and the fate was shared by 300 nm MAP (Figure S5B). An analysis of $\log_{10}(MSD_{\tau=1s})$ of 500 nm MAP unexpectedly revealed statistically significant differences between sCOPD versus Smoker or mCOPD groups (Figure S5C). However, median MSD values of 500 nm MAP measured in sputum samples from sCOPD patients were near the tracking resolution and thus these values cannot be reliably used to probe disease severity.

Based on all of these findings, subsequent microstructural analyses were conducted with 100 nm MIP. We first utilized the measured MSD values of 100 nm MIP, in conjunction with obstruction-scaling model [28], to estimate pore sizes of sputum samples. As expected from the

particle diffusion behaviors (Figure 3), we found that the fractions of smaller pores were clearly reduced with the increase in disease severity (Figure S6).

Sputum biochemical composition analysis

We hypothesized that biochemical composition might impact on the microstructural properties of sputum and, thus, we measured the macromolecular contents of the sputum samples. The percent solids in the sputum collected ranged from 1.1 – 6.5% by weight, with the higher values primarily associated with more severe disease. The solids content for samples from non-COPD smokers (N = 7) and COPD patients (N = 26) was 2.5 ± 0.5% and 3.1 ± 0.2% on average, respectively, which is in agreement with previously published values [22]. Sputum from sCOPD patients exhibited the highest percent solids content (3.4 ± 0.3%), while the percent solids for smoker and mCOPD samples were 2.5 ± 0.5% and 3.0 ± 0.3%, respectively (Figure 4A). We then found that the percent solids content values inversely correlated with the $\log_{10}$(median $MSD_{\tau=1s}$) of 100 nm MIP (Figure 5A; Spearman r = -0.73, $p < 0.0001$).

We next measured concentrations of the primary macromolecules found in sputum, specifically mucin and DNA, and investigated whether they correlated with the diffusion rates of 100 nm MIP. The mucin concentration was about 2-fold greater in the amassed COPD sputum samples compared to that from non-COPD smokers (5.5 ± 0.7 and 2.9 ± 0.6 mg/ml, respectively). Specifically, the sCOPD cohort possessed the highest sputum mucin concentration at 8.4 ± 1.9 mg/ml and was statistically significant compared with that of both the smokers (3.0 ± 0.6 mg/ml) and the mCOPD group (4.4 ± 0.6 mg/ml), respectively (Figure 4B, $p < 0.05$). However, the difference was not statistically significant between non-COPD smokers and mCOPD group. The DNA concentration was higher in amassed COPD sputum samples compared to the sample from smokers, averaging 0.21 ± 0.07 and 0.07 ± 0.01 mg/ml,

respectively, but the differences were not statistically significant among different groups (Figure 4C). When related to MIP diffusion, mucin concentration inversely correlated with the $\log_{10}$(median $MSD_{\tau=1s}$) of 100 nm MIP (Figure 5B; r = -0.41, p=0.03); however, the relationship was not statistically significant for DNA content and $\log_{10}$(median $MSD_{\tau=1s}$) of 100 nm MIP (Figure 5C; r = -0.18, p = 0.36).

Relationship between lung function and microstructure

We hypothesized that the altered sputum microstructure in COPD would correlate with impaired lung function. The $\log_{10}$(median $MSD_{\tau=1s}$) of 100 nm MIP was positively correlated with the spirometric measurements of FEV_{1s}/FVC (Figure 6A; r = 0.41, p = 0.02) and FEV_{1s}% predicted (Figure 6B; r = 0.41, p = 0.02). We also compared the spirometric measurements to the solids content which has been previously assessed as a potential biomarker for lung function of CB patients [22]. Neither the FEV_{1s}% predicted nor the FEV_{1s}/FVC % predicted significantly correlated with the sputum percent solids (Figures 6C, D).

Discussion

In this study, we examined whether sputum architecture, reflecting the pore size of spontaneously expectorated mucus gel, associates with COPD severity, lung function and sputum composition. To our knowledge, this is the first analysis of sputum microstructure in COPD patients. We specifically investigated the microstructural properties of spontaneously expectorated sputum from smokers with and without airway obstruction using MPT with MIP probes. We showed that dense surface coatings with low molecular weight PEG effectively prevented nanoparticle adhesion to sputum constituents, particularly mucins, similar to our

observations with other mucus secretions, including cervicovaginal mucus [35], respiratory mucus [36], chronic rhinosinusitis mucus [37], and CF sputum [38]. We also demonstrated that the diffusion rates of MIP possessing particle diameter less than the average sputum mesh size (100 nm MIP in this case) can be used to distinguish key biophysical properties of sputum collected from patients with varying disease severity. We found that a tightened microstructure correlated with lung disease severity as indicated by a decrease in in FEV_{1s}/FVC and FEV_{1s}. Finally, the mesh spacing (i.e. pore size) of the sputum network may impact the migration and/or colonization of microorganisms [39, 40], including bacteria and viruses, and immune cells. If so, the mesh spacing measurement can potentially serve as a predictor of COPD-associated exacerbation, a critical risk factor for COPD progression [41].

Sputum is a gel that is composed of a complex porous network of solid strands of mucins, DNA and other molecules in an aqueous medium. In order to accurately perform microstructural analysis of the sputum mesh via MPT, the nanoparticle probes must be both non-adhesive and smaller than the average pore size in the sputum mesh [26]. Transport rates of MAP are strongly affected by adhesive interactions with the sputum, whereas MIP resist adhesive interactions with sputum constituents. Due to their muco-inert nature, MIP movement is primarily affected by steric hindrance imposed by the sputum mesh, which makes MIP uniquely appropriate for use in examination of unperturbed sputum architecture, such as mesh spacing. We found that 100 nm MIP traveled relatively unhindered through the porous sputum samples freshly obtained from both non-COPD smokers and COPD patients. In contrast, 500 nm MIP, despite their muco-inert surfaces, did not diffuse rapidly in sputum because they are too large to fit through the sputum pores. These findings indicate that 100 nm MIP are optimal to probe the sputum microstructure, whereas conventional MAP of any size and MIP larger than the average opening size in the sputum mesh are not suitable for this application.

Biophysical properties of COPD sputum have been relatively underexplored compared to biochemical content analysis, including quantification of pro-inflammatory and bacterial cell markers [42, 43]. Previous biophysical analysis of sputum samples collected from patients with obstructive lung diseases primarily focused on measurement and comparison of macro-rheological properties; for example, the degree of purulence, an indication of infection, was correlated with bulk viscoelasticity of CF sputum [25]. However, these conventional rheological measurements do not provide direct information on sputum microarchitecture [33, 44]. By combining MIP and the MPT technique to probe sputum microstructure, we discovered a significant correlation between diffusion of 100 nm MIP and disease stage, specifically between sputum samples from smokers and sCOPD patients. The reduction in MIP diffusion rates, as quantified by $\log_{10}$(median $MSD_{\tau=1s}$), indicates that the sputum mesh (i.e. pore size) is tighter in sputum samples from more advanced COPD.

Consistent with previous reports [22, 23], we found a modest increase in the percent solids content of sputum samples from COPD patients, especially sCOPD, compared with that of smokers. We found an inverse correlation between percent solids and the MIP $\log_{10}$(median $MSD_{\tau=1s}$), suggesting that a greater solids concentration, as can occur with sputum dehydration [23] or mucin hypersecretion, contributes to a tighter sputum mesh in severe COPD. This agrees with a previous report where *in vitro* particle diffusion rates in mucus inversely correlated with solids content [22]. However, this study was conducted with large (1 μm), non-PEGylated (muco-adhesive) particles and, thus, the diffusion readout is more relevant to bulk rheological mucus properties than to microstructural properties such as pore size [45].

Many believe that airway inflammation in obstructive lung disease is linked to perturbation of mucin [46] and/or DNA content [47], which results in elevation of mucus elasticity [8, 48]. We found that the mucin concentration was significantly increased in sputum samples collected from COPD patients compared to the samples from non-COPD smokers. This is in

agreement with a recently published paper that demonstrated that the total mucin concentration was significantly higher in induced sputum from patients diagnosed with CB compared to those without CB [49]. Indeed, we found that the increased mucin concentration corresponded with a tighter sputum microstructure in this study. The pore size of the mucus mesh can potentially be affected by the crosslinking density of mucin fibers [48, 50]. Yuan and coworkers recently reported that oxidation arising from airway inflammation increases the number of disulfide crosslinks of mucin polymers and, thus, increases the stiffness/elasticity of CF sputum [48]. Increased oxidative stress is also a hallmark of COPD-associated lung disease [51, 52]. We also note that other biochemical properties, including pH and salt composition, may affect molecular arrangements of macromolecules, thereby impacting on mucus biophysical properties [53, 54].

We found for the first time that sputum microstructural properties correlated with lung function measures (i.e. FEV_{1s}/FVC and FEV_{1s} % predicted) in COPD. In CF sputum, altered sputum rheological properties correlate with bacterial colonization and reduced lung function [55]. The tighter mesh in COPD sputum may also provide a permissive environment for chronic infection and inflammation, perhaps due to reduced bacteria and neutrophil migration coupled with reduced MCC [39]. Thus, microstructure readouts based on MIP diffusion in sputum may inform the study of disease progression and/or clinical exacerbations. Importantly, there is not a significant relationship between lung function and percent solids potentially limiting the solids content as a biomarker for COPD severity. Further, the microstructure analysis may also be implemented as a readout in therapeutic trials to evaluate airway-directed therapies, including mucolytic and mucus-hydrating agents [56]. Finally, our findings invite further analysis of the molecular interactions that contribute to pore size such as disulfide cross-linking, oxidative modifications and mucin-macromolecule interactions. The microstructure measurement can only be performed on fresh, spontaneously expectorated sputum in order to preserve the

physiological structure and to prevent deterioration observed with prolonged storage or freezing [28]. Induced sputum samples were not used since dilution by inhaled saline during the collection process may alter the physiological microstructure. Thus, the COPD patient population sampled with this method is constrained by the ability to generate a spontaneous specimen.

Overall, our findings suggest that the characterization of sputum microstructure, available with spontaneous but not induced sputum samples, may provide novel insights into the specific properties of mucus that contribute to COPD pathogenesis. Future studies will focus on the examination of sputum architecture in larger longitudinal cohorts with detailed clinical, physiologic and functional readouts. Such studies could further support the use of sputum mesh size as a predictive and personalized index of disease state and progression.

Acknowledgements

This work was supported by the National Institutes of Health (R01HL127413 and R01HL125169) and the Cystic Fibrosis Foundation. The content is solely the responsibility of the authors and does not necessarily represent the official views of the National Institutes of Health. The authors thank the SPIROMICS participants and participating physicians, investigators and staff for making this research possible. More information about the study and how to access SPIROMICS data is available at www.spiromics.org. We would like to acknowledge the following current and former investigators of the SPIROMICS sites and reading centers: Neil E Alexis, PhD; Wayne H Anderson, PhD; R Graham Barr, MD, DrPH; Eugene R Bleecker, MD; Richard C Boucher, MD; Russell P Bowler, MD, PhD; Elizabeth E Carretta, MPH; Stephanie A Christenson, MD; Alejandro P Comellas, MD; Christopher B Cooper, MD, PhD; David J Couper, PhD; Gerard J Criner, MD; Ronald G Crystal, MD; Jeffrey L Curtis, MD; Claire M Doerschuk, MD; Mark T Dransfield, MD; Christine M Freeman, PhD; MeiLan K Han, MD, MS; Nadia N Hansel, MD, MPH; Annette T Hastie, PhD; Eric A Hoffman, PhD; Robert J Kaner, MD; Richard E Kanner, MD; Eric C Kleerup, MD; Jerry A Krishnan, MD, PhD; Lisa M LaVange, PhD; Stephen C Lazarus, MD; Fernando J Martinez, MD, MS; Deborah A Meyers, PhD; John D Newell Jr, MD; Elizabeth C Oelsner, MD, MPH; Wanda K O'Neal, PhD; Robert Paine, III, MD; Nirupama Putcha, MD, MHS; Stephen I. Rennard, MD; Donald P Tashkin, MD; Mary Beth Scholand, MD; J Michael Wells, MD; Robert A Wise, MD; and Prescott G Woodruff, MD, MPH. The project officers from the Lung Division of the National Heart, Lung, and Blood Institute were Lisa Postow, PhD, and Thomas Croxton, PhD, MD. SPIROMICS was supported by contracts from the NIH/NHLBI (HHSN268200900013C, HHSN268200900014C, HHSN268200900015C, HHSN268200900016C, HHSN268200900017C, HHSN268200900018C HHSN268200900019C, HHSN268200900020C), which were supplemented by contributions made through the Foundation for the NIH from AstraZeneca;

Bellerophon Pharmaceuticals; Boehringer-Ingelheim Pharmaceuticals, Inc; Chiesi Farmaceutici SpA; Forest Research Institute, Inc; GSK; Grifols Therapeutics, Inc; Ikaria, Inc; Nycomed GmbH; Takeda Pharmaceutical Company; Novartis Pharmaceuticals Corporation; Regeneron Pharmaceuticals, Inc; and Sanofi.

Competing interests:

The muco-inert particle technology described in this publication is being developed by Kala Pharmaceuticals. J.H. declares a financial, a management/advisor, and a paid consulting relationship with Kala Pharmaceuticals. J.H. is a cofounder of Kala Pharmaceuticals and owns company stock, which is subject to certain restrictions under Johns Hopkins University policy. The terms of this arrangement are being managed by Johns Hopkins University in accordance with its conflict-of-interest policies.

References

1. Rogers DF. Mucus hypersecretion in chronic obstructive pulmonary disease. *Novartis Foundation symposium* 2001: 234: 65-77; discussion 77-83.
2. Cerveri I, Brusasco V. Revisited role for mucus hypersecretion in the pathogenesis of COPD. *European respiratory review : an official journal of the European Respiratory Society* 2010: 19(116): 109-112.
3. Kreda SM, Davis CW, Rose MC. CFTR, mucins, and mucus obstruction in cystic fibrosis. *Cold Spring Harbor perspectives in medicine* 2012: 2(9): a009589.
4. Evans CM, Kim K, Tuvim MJ, Dickey BF. Mucus hypersecretion in asthma: causes and effects. *Current opinion in pulmonary medicine* 2009: 15(1): 4-11.
5. Hoyert DL, Xu J. Deaths: preliminary data for 2011. *National vital statistics reports : from the Centers for Disease Control and Prevention, National Center for Health Statistics, National Vital Statistics System* 2012: 61(6): 1-51.
6. Kim V, Han MK, Vance GB, Make BJ, Newell JD, Hokanson JE, Hersh CP, Stinson D, Silverman EK, Criner GJ. The chronic bronchitic phenotype of COPD: an analysis of the COPDGene Study. *Chest* 2011: 140(3): 626-633.
7. Marsh SE, Travers J, Weatherall M, Williams MV, Aldington S, Shirtcliffe PM, Hansell AL, Nowitz MR, McNaughton AA, Soriano JB, Beasley RW. Proportional classifications of COPD phenotypes. *Thorax* 2008: 63(9): 761-767.
8. Fahy JV, Dickey BF. Airway mucus function and dysfunction. *The New England journal of medicine* 2010: 363(23): 2233-2247.
9. Knowles MR, Boucher RC. Mucus clearance as a primary innate defense mechanism for mammalian airways. *The Journal of clinical investigation* 2002: 109(5): 571-577.
10. Schneider CS, Xu Q, Boylan NJ, Chisholm J, Tang BC, Schuster BS, Henning A, Ensign LM, Lee E, Adstamongkonkul P, Simons BW, Wang SS, Gong X, Yu T, Boyle MP, Suk JS, Hanes J. Nanoparticles that do not adhere to mucus provide uniform and long-lasting drug delivery to airways following inhalation. *Sci Adv* 2017: 3(4): e1601556.
11. Danahay H, Jackson AD. Epithelial mucus-hypersecretion and respiratory disease. *Current drug targets Inflammation and allergy* 2005: 4(6): 651-664.
12. Allinson JP, Hardy R, Donaldson GC, Shaheen SO, Kuh D, Wedzicha JA. The Presence of Chronic Mucus Hypersecretion Across Adult Life in Relation to COPD Development. *American journal of respiratory and critical care medicine* 2015.
13. Vestbo J, Prescott E, Lange P. Association of chronic mucus hypersecretion with FEV1 decline and chronic obstructive pulmonary disease morbidity. Copenhagen City Heart Study Group. *American journal of respiratory and critical care medicine* 1996: 153(5): 1530-1535.
14. Hogg JC, Chu F, Utokaparch S, Woods R, Elliott WM, Buzatu L, Cherniack RM, Rogers RM, Sciurba FC, Coxson HO, Pare PD. The nature of small-airway obstruction in chronic obstructive pulmonary disease. *The New England journal of medicine* 2004: 350(26): 2645-2653.
15. Hogg JC, Chu FS, Tan WC, Sin DD, Patel SA, Pare PD, Martinez FJ, Rogers RM, Make BJ, Criner GJ, Cherniack RM, Sharafkhaneh A, Luketich JD, Coxson HO, Elliott WM, Sciurba FC. Survival after lung volume reduction in chronic obstructive pulmonary disease: insights from small airway pathology. *American journal of respiratory and critical care medicine* 2007: 176(5): 454-459.
16. Burgel PR, Nesme-Meyer P, Chanez P, Caillaud D, Carre P, Perez T, Roche N. Cough and sputum production are associated with frequent exacerbations and hospitalizations in COPD subjects. *Chest* 2009: 135(4): 975-982.

17. Corhay JL, Vincken W, Schlesser M, Bossuyt P, Imschoot J. Chronic bronchitis in COPD patients is associated with increased risk of exacerbations: a cross-sectional multicentre study. *International journal of clinical practice* 2013: 67(12): 1294-1301.
18. Hurst JR, Vestbo J, Anzueto A, Locantore N, Mullerova H, Tal-Singer R, Miller B, Lomas DA, Agusti A, Macnee W, Calverley P, Rennard S, Wouters EF, Wedzicha JA, Evaluation of CLtIPSEI. Susceptibility to exacerbation in chronic obstructive pulmonary disease. *The New England journal of medicine* 2010: 363(12): 1128-1138.
19. Williams OW, Sharafkhaneh A, Kim V, Dickey BF, Evans CM. Airway mucus: From production to secretion. *American journal of respiratory cell and molecular biology* 2006: 34(5): 527-536.
20. Randell SH, Boucher RC. Effective mucus clearance is essential for respiratory health. *American journal of respiratory cell and molecular biology* 2006: 35(1): 20-28.
21. Caramori G, Di Gregorio C, Carlstedt I, Casolari P, Guzzinati I, Adcock IM, Barnes PJ, Ciaccia A, Cavallesco G, Chung KF, Papi A. Mucin expression in peripheral airways of patients with chronic obstructive pulmonary disease. *Histopathology* 2004: 45(5): 477-484.
22. Hill DB, Vasquez PA, Mellnik J, McKinley SA, Vose A, Mu F, Henderson AG, Donaldson SH, Alexis NE, Boucher RC, Forest MG. A biophysical basis for mucus solids concentration as a candidate biomarker for airways disease. *PloS one* 2014: 9(2): e87681.
23. Anderson WH, Coakley RD, Button B, Henderson AG, Zeman KL, Alexis NE, Peden DB, Lazarowski ER, Davis CW, Bailey S, Fuller F, Almond M, Qaqish B, Bordonali E, Rubinstein M, Bennett WD, Kesimer M, Boucher RC. The Relationship of Mucus Concentration (Hydration) to Mucus Osmotic Pressure and Transport in Chronic Bronchitis. *American journal of respiratory and critical care medicine* 2015.
24. Giordano AM, Holsclaw D, Litt M. Mucus rheology and mucociliary clearance: Normal physiologic state. *The American review of respiratory disease* 1978: 118(2): 245-250.
25. Serisier DJ, Carroll MP, Shute JK, Young SA. Macrorheology of cystic fibrosis, chronic obstructive pulmonary disease & normal sputum. *Respiratory research* 2009: 10: 63.
26. Lai SK, Wang YY, Wirtz D, Hanes J. Micro- and macrorheology of mucus. *Advanced drug delivery reviews* 2009: 61(2): 86-100.
27. Duncan GA, Jung J, Hanes J, Suk JS. The Mucus Barrier to Inhaled Gene Therapy. *Mol Ther* 2016: 24(12): 2043-2053.
28. Duncan GA, Jung J, Joseph A, Thaxton AL, West NE, Boyle MP, Hanes J, Suk JS. Microstructural alterations of sputum in cystic fibrosis lung disease. *JCI Insight* 2016: 1(18): e88198.
29. Suk JS, Xu Q, Kim N, Hanes J, Ensign LM. PEGylation as a strategy for improving nanoparticle-based drug and gene delivery. *Advanced drug delivery reviews* 2016: 99(Pt A): 28-51.
30. Xu Q, Boylan NJ, Suk JS, Wang YY, Nance EA, Yang JC, McDonnell PJ, Cone RA, Duh EJ, Hanes J. Nanoparticle diffusion in, and microrheology of, the bovine vitreous ex vivo. *Journal of controlled release : official journal of the Controlled Release Society* 2013: 167(1): 76-84.
31. Nance EA, Woodworth GF, Sailor KA, Shih TY, Xu Q, Swaminathan G, Xiang D, Eberhart C, Hanes J. A dense poly(ethylene glycol) coating improves penetration of large polymeric nanoparticles within brain tissue. *Science translational medicine* 2012: 4(149): 149ra119.
32. Nance E, Zhang C, Shih TY, Xu Q, Schuster BS, Hanes J. Brain-penetrating nanoparticles improve paclitaxel efficacy in malignant glioma following local administration. *ACS nano* 2014: 8(10): 10655-10664.
33. Schuster BS, Ensign LM, Allan DB, Suk JS, Hanes J. Particle tracking in drug and gene delivery research: State-of-the-art applications and methods. *Advanced drug delivery reviews* 2015.
34. Mastorakos P, da Silva AL, Chisholm J, Song E, Choi WK, Boyle MP, Morales MM, Hanes J, Suk JS. Highly compacted biodegradable DNA nanoparticles capable of overcoming the mucus barrier for inhaled lung gene therapy. *Proceedings of the National Academy of Sciences of the United States of America* 2015: 112(28): 8720-8725.

35. Lai SK, O'Hanlon DE, Harrold S, Man ST, Wang YY, Cone R, Hanes J. Rapid transport of large polymeric nanoparticles in fresh undiluted human mucus. *Proceedings of the National Academy of Sciences of the United States of America* 2007: 104(5): 1482-1487.
36. Schuster BS, Suk JS, Woodworth GF, Hanes J. Nanoparticle diffusion in respiratory mucus from humans without lung disease. *Biomaterials* 2013: 34(13): 3439-3446.
37. Lai SK, Suk JS, Pace A, Wang YY, Yang M, Mert O, Chen J, Kim J, Hanes J. Drug carrier nanoparticles that penetrate human chronic rhinosinusitis mucus. *Biomaterials* 2011: 32(26): 6285-6290.
38. Suk JS, Lai SK, Wang YY, Ensign LM, Zeitlin PL, Boyle MP, Hanes J. The penetration of fresh undiluted sputum expectorated by cystic fibrosis patients by non-adhesive polymer nanoparticles. *Biomaterials* 2009: 30(13): 2591-2597.
39. Matsui H, Verghese MW, Kesimer M, Schwab UE, Randell SH, Sheehan JK, Grubb BR, Boucher RC. Reduced three-dimensional motility in dehydrated airway mucus prevents neutrophil capture and killing bacteria on airway epithelial surfaces. *J Immunol* 2005: 175(2): 1090-1099.
40. Bansil R, Celli JP, Hardcastle JM, Turner BS. The Influence of Mucus Microstructure and Rheology in Helicobacter pylori Infection. *Frontiers in immunology* 2013: 4: 310.
41. Ramsey SD, Hobbs FD. Chronic obstructive pulmonary disease, risk factors, and outcome trials: comparisons with cardiovascular disease. *Proceedings of the American Thoracic Society* 2006: 3(7): 635-640.
42. Paone G, Conti V, Vestri A, Leone A, Puglisi G, Benassi F, Brunetti G, Schmid G, Cammarella I, Terzano C. Analysis of sputum markers in the evaluation of lung inflammation and functional impairment in symptomatic smokers and COPD patients. *Disease markers* 2011: 31(2): 91-100.
43. Bartoli ML, Di Franco A, Vagaggini B, Bacci E, Cianchetti S, Dente FL, Tonelli M, Paggiaro PL. Biological markers in induced sputum of patients with different phenotypes of chronic airway obstruction. *Respiration; international review of thoracic diseases* 2009: 77(3): 265-272.
44. Ensign LM, Schneider C, Suk JS, Cone R, Hanes J. Mucus Penetrating Nanoparticles: Biophysical Tool and Method of Drug and Gene Delivery. *Adv Mater* 2012: 24(28): 3887-3894.
45. Mason TG, Ganesan K, vanZanten JH, Wirtz D, Kuo SC. Particle tracking microrheology of complex fluids. *Phys Rev Lett* 1997: 79(17): 3282-3285.
46. Hauber HP, Foley SC, Hamid Q. Mucin overproduction in chronic inflammatory lung disease. *Canadian respiratory journal* 2006: 13(6): 327-335.
47. Wright TK, Gibson PG, Simpson JL, McDonald VM, Wood LG, Baines KJ. Neutrophil extracellular traps are associated with inflammation in chronic airway disease. *Respirology* 2016: 21(3): 467-475.
48. Yuan S, Hollinger M, Lachowicz-Scroggins ME, Kerr SC, Dunican EM, Daniel BM, Ghosh S, Erzurum SC, Willard B, Hazen SL, Huang X, Carrington SD, Oscarson S, Fahy JV. Oxidation increases mucin polymer cross-links to stiffen airway mucus gels. *Science translational medicine* 2015: 7(276): 276ra227.
49. Kesimer M, Ford AA, Ceppe A, Radicioni G, Cao R, Davis CW, Doerschuk CM, Alexis NE, Anderson WH, Henderson AG, Barr RG, Bleecker ER, Christenson SA, Cooper CB, Han MK, Hansel NN, Hastie AT, Hoffman EA, Kanner RE, Martinez F, Paine R, 3rd, Woodruff PG, O'Neal WK, Boucher RC. Airway Mucin Concentration as a Marker of Chronic Bronchitis. *The New England journal of medicine* 2017: 377(10): 911-922.
50. Nielsen H, Hvidt S, Sheils CA, Janmey PA. Elastic contributions dominate the viscoelastic properties of sputum from cystic fibrosis patients. *Biophysical chemistry* 2004: 112(2-3): 193-200.
51. Repine JE, Bast A, Lankhorst I. Oxidative stress in chronic obstructive pulmonary disease. Oxidative Stress Study Group. *American journal of respiratory and critical care medicine* 1997: 156(2 Pt 1): 341-357.
52. Kirkham PA, Barnes PJ. Oxidative stress in COPD. *Chest* 2013: 144(1): 266-273.

53. Tang XX, Ostedgaard LS, Hoegger MJ, Moninger TO, Karp PH, McMenimen JD, Choudhury B, Varki A, Stoltz DA, Welsh MJ. Acidic pH increases airway surface liquid viscosity in cystic fibrosis. *J Clin Invest* 2016: 126(3): 879-891.
54. Wang YY, Lai SK, Ensign LM, Zhong W, Cone R, Hanes J. The microstructure and bulk rheology of human cervicovaginal mucus are remarkably resistant to changes in pH. *Biomacromolecules* 2013: 14(12): 4429-4435.
55. Tomaiuolo G, Rusciano G, Caserta S, Carciati A, Carnovale V, Abete P, Sasso A, Guido S. A new method to improve the clinical evaluation of cystic fibrosis patients by mucus viscoelastic properties. *PloS one* 2014: 9(1): e82297.
56. Braga PC, Allegra L, Bossi R, Guffanti EE, Scarpazza G, Bisetti A, Spada E, Fumagalli G. Identification of subpopulations of bronchitic patients for suitable therapy by a dynamic rheological test. *International journal of clinical pharmacology research* 1989: 9(3): 175-182.

Figure Legends

Figure 1. Transport of MAP and MIP in spontaneously expectorated sputum from cigarette smokers without COPD. (**A**) Representative median trajectories of MAP and MIP possessing particle diameters of 100, 300, and 500 nm. Trajectories show 15 seconds of motion. Scale bar = 2 μm. (**B-D**) Median mean squared displacement (MSD) at a time scale of 1 second for MAP and MIP with diameters of (**B**) 100 nm, (**C**) 300 nm, and (**D**) 500 nm. All data represents N = 7 sputum samples with at least 500 particles tracked per sample. Error bars represent SEM. *$p < 0.05$ (Wilcoxon signed rank test).

Figure 2. Transport of MAP and MIP in spontaneously expectorated sputum from COPD patients. (**A**) Representative trajectories of MAP and MIP possessing particle diameters of 100, 300, and 500 nm. Trajectories show 15 seconds of motion. Scale bar = 2 μm. Median MSD at a time scale of 1 second for MAP and MIP with diameters of (**B**) 100 nm, (**C**) 300 nm, and (**D**) 500 nm. All data represents N ≥ 13 sputum samples with at least 500 particles tracked per sample. Error bars represent SEM. **$p < 0.01$, ***$p < 0.001$ (Wilcoxon signed rank test).

Figure 3. Transport of differently sized MIP in spontaneously expectorated sputum from non-COPD smokers and COPD patients stratified for disease severity based on spirometric pulmonary function measurements. Subjects are categorized into one of the three groups, including non-COPD cigarette smokers (Smoker), mild COPD (mCOPD) and severe COPD (sCOPD). Distribution of the $\log_{10}(MSD_{\tau=1s})$ of individual MIP possessing particle diameters of (**A**) 100 nm, (**B**) 300 nm and (**C**) 500 nm. All data represents N ≥ 5 sputum samples with at least 500 particles tracked per sample. The median values of $\log_{10}(MSD_{\tau=1s})$ for

each data set is indicated by the dashed line. Black bar represents values below tracking resolution.

Figure 4. Sputum biochemical contents. Quantification of (**A**) percent solids (**B**) mucin concentration and (**C**) DNA concentration in sputum samples from smokers without COPD (Smoker), patients with mild COPD (mCOPD) and severe COPD (sCOPD). Data represents N ≥ 29 sputum samples. Error bars represent SEM. *Denotes statistically significant differences ($p < 0.05$, ANOVA)

Figure 5. Relationships between sputum microstructure and biochemical components. Log_{10}(median $MSD_{\tau=1s}$) values of 100 nm MIP inversely correlates with (**A**) percent solids content and (**B**) mucin concentration but not (**C**) DNA concentration. Measurements were made for N ≥ 28 individual, non-overlapping non-COPD smokers and COPD patients.

Figure 6. Relationships between sputum microstructure and spirometric measurements. Log_{10}(median $MSD_{\tau=1s}$) values of 100 nm MIP positively correlates with (**A**) the ratio of post-bronchodilator FEV_{1s} to FVC ratio and (**B**) post-bronchodilator FEV_{1s} % predicted, but the percent solids and (**C**) FEV_{1s} % predicted or (**D**) FEV_{1s} to FVC ratio are not correlated. Spirometry was performed on patients prior to sputum collection. Measurements were made for N ≥ 30 individual, non-overlapping non-COPD smokers and COPD patients.

Table 1. Participant demographics

	Smoker $FEV_{1s}/FVC>0.7$ $FVC>LLN$[a]	Mild-moderate COPD $FEV_{1s}/FVC<0.7$ $FEV_{1s}>50\%$ pred	Moderate-severe COPD $FEV_{1s}/FVC<0.7$ $FEV_{1s}<50\%$ pred
N	7	18	8
Age	56 ± 2	62 ± 2	70 ± 3
Post-BD[b] FEV_{1s} (% predicted)	95 ± 7	69 ± 4	39 ± 2
FEV_{1s}/FVC	0.97 ± 0.02	0.78 ± 0.02	0.5 ± 0.04
Female, n (%)	3 (43%)	9 (49%)	1 (17%)
Current smoker, n (%)	5 (71%)	12 (67%)	4 (67%)

[a] lower limit of normal

[b] post-bronchodilator

Values displayed as mean ± SEM unless otherwise indicated.

Table 2. Nanoparticle physicochemical characterization

Nominal Size (nm)	Particle Type	Hydrodynamic Diameter[a] (nm)	PDI[a]	ζ–potential[b] (mV)
100	MAP	88 ± 1	0.02	-52 ± 1
100	MIP	109 ± 2	0.02	-7 ± 1
300	MAP	292 ± 4	0.01	-75 ± 6
300	MIP	318 ± 7	0.04	-4 ± 1
500	MAP	538 ± 11	0.05	-52 ± 1
500	MIP	553 ± 5	0.05	-4 ± 1

[a] Hydrodynamic diameter and polydispersity index (PDI) measured in 10 mM NaCl at pH 7.4 by dynamic light scattering. Values displayed as mean ± SEM.

[b] Measured in 10 mM NaCl at pH 7.4. Values displayed as mean ± SEM.

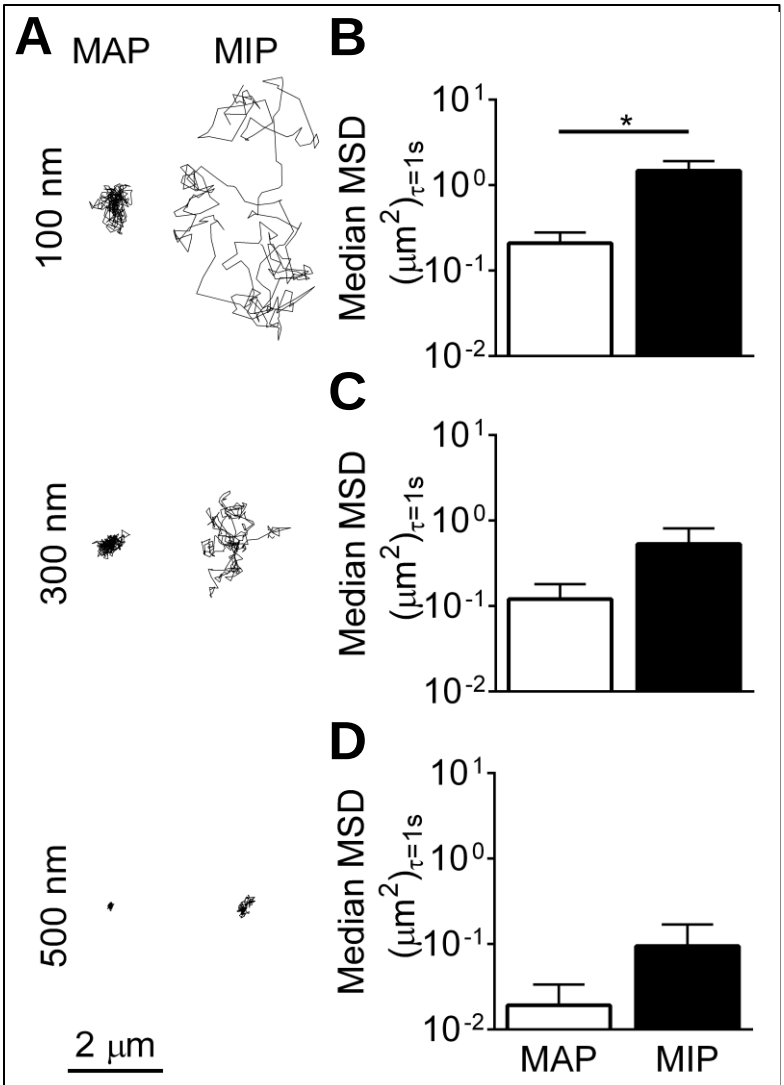

Figure 1. Transport of MAP and MIP in spontaneously expectorated sputum from cigarette smokers without COPD. (**A**) Representative median trajectories of MAP and MIP possessing particle diameters of 100, 300, and 500 nm. Trajectories show 15 seconds of motion. Scale bar = 2 μm. (**B-D**) Median mean squared displacement (MSD) at a time scale of 1 second for MAP and MIP with diameters of (**B**) 100 nm, (**C**) 300 nm, and (**D**) 500 nm. All data represents N = 7 sputum samples with at least 500 particles tracked per sample. Error bars represent SEM. *$p < 0.05$ (Wilcoxon signed rank test).

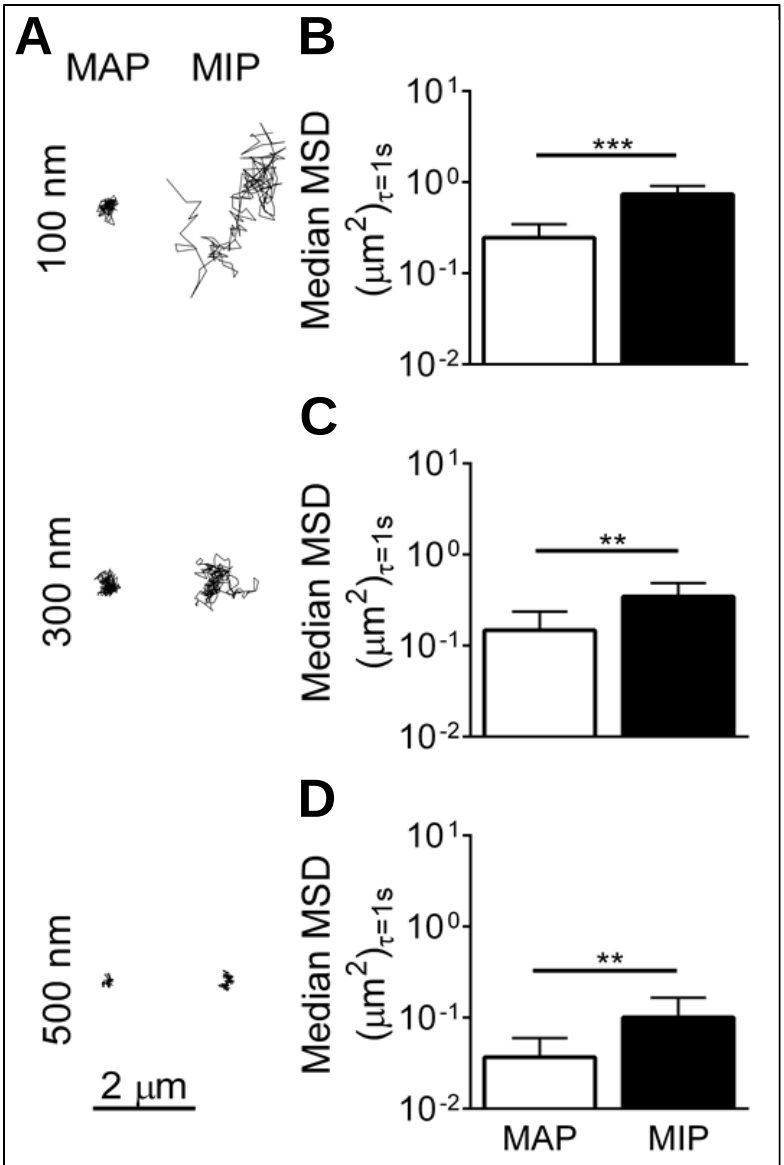

Figure 2. Transport of MAP and MIP in spontaneously expectorated sputum from COPD patients. (**A**) Representative trajectories of MAP and MIP possessing particle diameters of 100, 300, and 500 nm. Trajectories show 15 seconds of motion. Scale bar = 2 μm. Median MSD at a time scale of 1 second for MAP and MIP with diameters of (**B**) 100 nm, (**C**) 300 nm, and (**D**) 500 nm. All data represents N ≥ 13 sputum samples with at least 500 particles tracked per sample. Error bars represent SEM. $^{**}p < 0.01$, $^{***}p < 0.001$ (Wilcoxon signed rank test).

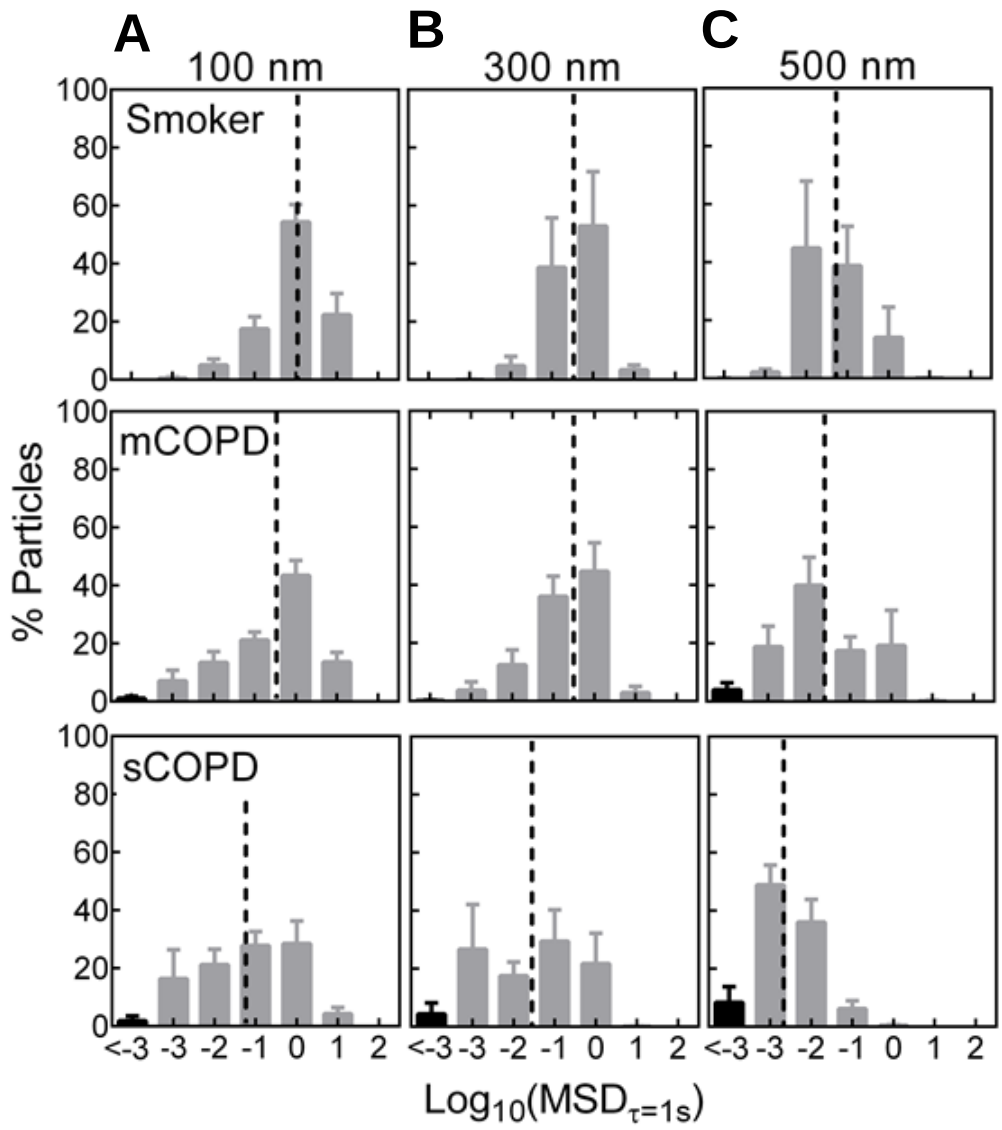

Figure 3. Transport of differently sized MIP in spontaneously expectorated sputum from non-COPD smokers and COPD patients stratified for disease severity based on spirometric pulmonary function measurements.
Subjects are categorized into one of the three groups, including non-COPD cigarette smokers (Smoker), mild COPD (mCOPD) and severe COPD (sCOPD). Distribution of the $\log_{10}(MSD_{\tau=1s})$ of individual MIP possessing particle diameters of (**A**) 100 nm, (**B**) 300 nm and (**C**) 500 nm. All data represents N ≥ 5 sputum samples with at least 500 particles tracked per sample. The median values of $\log_{10}(MSD_{\tau=1s})$ for each data set is indicated by the dashed line. Black bar represents values below tracking resolution.

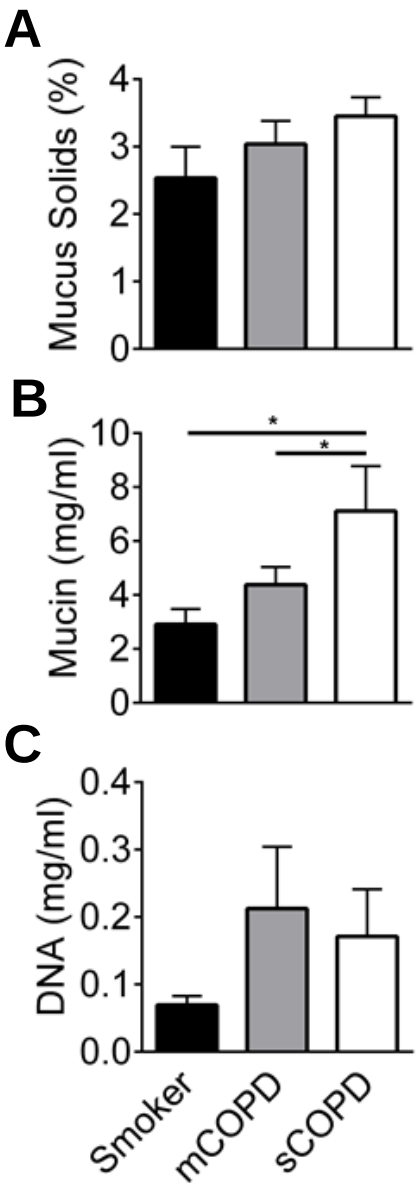

Figure 4. Sputum biochemical contents. Quantification of (**A**) percent solids (**B**) mucin concentration and (**C**) DNA concentration in sputum samples from smokers without COPD (Smoker), patients with mild COPD (mCOPD) and severe COPD (sCOPD). Data represents N ≥ 29 sputum samples. Error bars represent SEM. *Denotes statistically significant differences ($p < 0.05$, ANOVA)

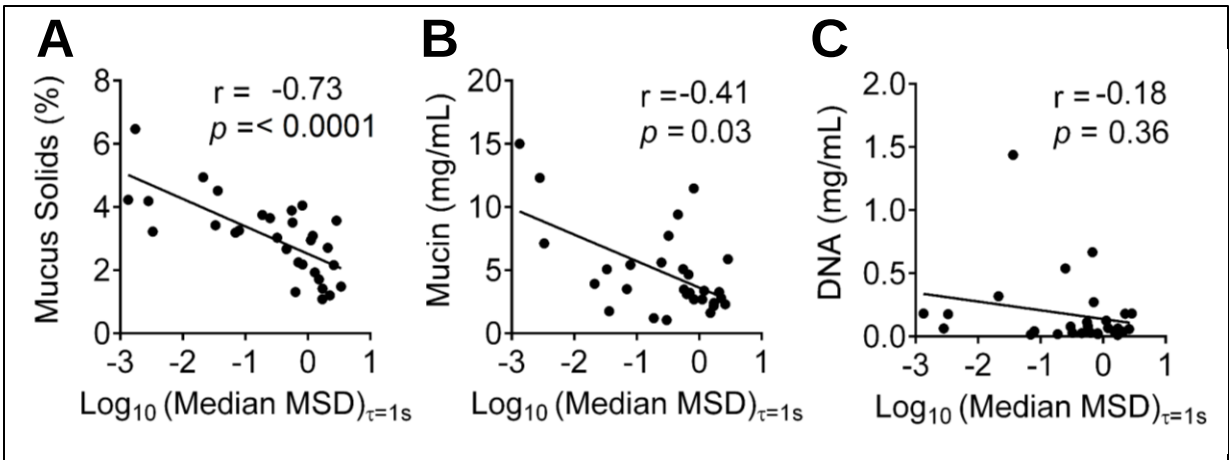

Figure 5. Relationships between sputum microstructure and biochemical components. Log_{10}(median $MSD_{\tau=1s}$) values of 100 nm MIP inversely correlates with (**A**) percent solids content and (**B**) mucin concentration but not (**C**) DNA concentration. Measurements were made for N ≥ 28 individual, non-overlapping non-COPD smokers and COPD patients.

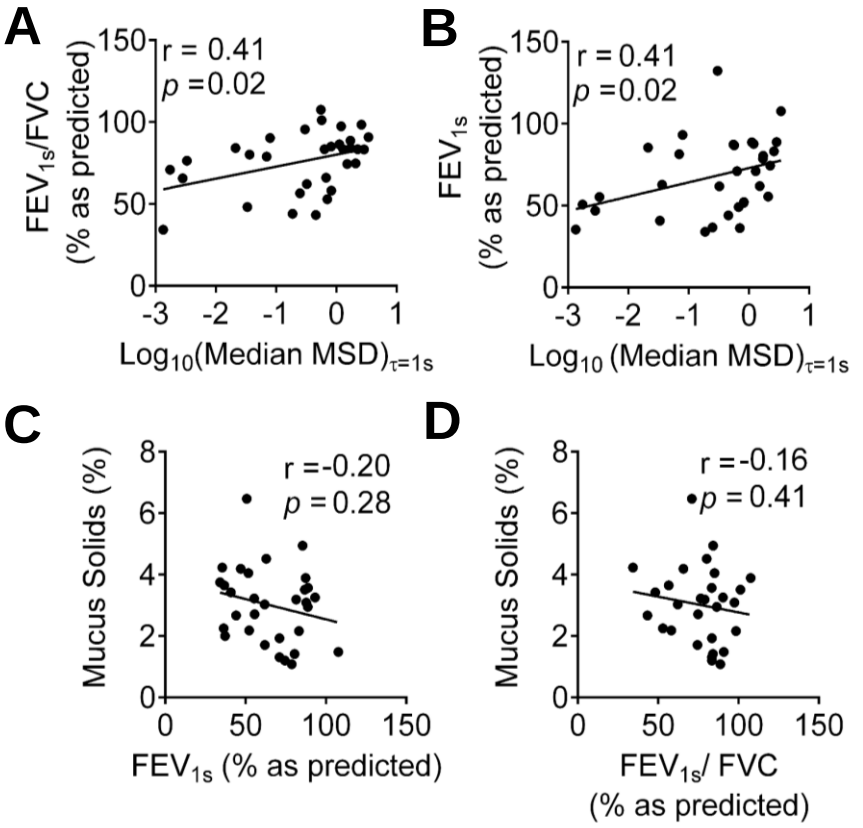

Figure 6. Relationships between sputum microstructure and spirometric measurements. Log_{10}(median $MSD_{\tau=1s}$) values of 100 nm MIP positively correlates with (**A**) the ratio of post-bronchodilator FEV_{1s} to FVC ratio and (**B**) post-bronchodilator FEV_{1s} % predicted, but the percent solids and (**C**) FEV_{1s} % predicted or (**D**) FEV_{1s} to FVC ratio are not correlated. Spirometry was performed on patients prior to sputum collection. Measurements were made for N ≥ 30 individual, non-overlapping non-COPD smokers and COPD patients.

Nanoparticle diffusion in spontaneously expectorated sputum as a biophysical tool to probe disease severity in COPD

Jane F. Chisholm[1,2], Siddharth K. Shenoy[1,7], Julie K. Shade[1,3], Victor Kim[4], Nirupama Putcha[5], Kathryn A. Carson[6], Robert Wise[5], Nadia N. Hansel[5], Justin S. Hanes[1-3,7†], Jung Soo Suk[1,7†], and Enid Neptune[5†]

Online Data Supplement

Supplemental Methods

Participant Demographics

Subpopulations and Intermediate Outcomes in COPD Study (SPIROMICS) is a multi-center longitudinal, observational study to identify novel phenotypes and biomarkers of COPD (1). Smokers (pack years ≥20 years) with or without airway obstruction were pre-stratified into three categories based on spirometric pulmonary function measurements, specifically forced expiratory volume in 1 second (FEV_{1s}) and forced vital capacity (FVC): cigarette smokers without airways obstruction (Smoker, FEV_{1s}/FVC>0.70, FVC>LLN), mild-moderate COPD (mCOPD, FEV_{1s}/FVC<0.70, FEV_{1s}>50%), and severe COPD (sCOPD, FEV_{1s}/FVC<0.70, FEV_{1s}<50%). For our study specifically, participants were asked to provide an expectorated sputum sample if possible at the same time as one of their annual scheduled SPIROMICS visits before providing an induced sample. Participants rinsed their mouths with water and after a deep breath with slow exhalation used a coughing manoeuvre to produce a deep sputum sample. Samples were stored at 4°C and analyzed by MPT within 24 h of collection in order to minimize sample degradation and alteration (2). Aliquots used to determine mucin and DNA content were frozen at -80°C until use. Additionally, as part of the SPIROMICS visit, participants filled out questionnaires to assess dyspnea with the modified Medical Research Council (MMRC) (3), severity of COPD (Body mass index, airflow Obstruction, Dyspnea and Exercise

capacity; BODE index) (4), and quality of life via the St. George's Respiratory Questionnaire (SGRQ) (5), the Short Form 12-item survey (SF-12) (6), and the COPD Assessment Test (CAT) score (7). Further, exercise capacity by the 6-minute walk distance (6MWD) and computed tomography (CT) measures of % gas trapping and % emphysema scans were measured.

Nanoparticle preparation and characterization

Fluorescent, carboxylate-modified polystyrene particles (PSCOOH; mucoadhesive particle or MAP) ranging in size from 100-500 nm were purchased from Life Technologies (Carlsbad, CA). PEG-modified particles (PSPEG; muco-inert particle or MIP) were prepared by covalently conjugating 5 kDa methoxy-PEG-amine (Creative PEGworks, Winston Salem, NC) to the carboxyl groups on the PSCOOH particles using carbodiimide coupling chemistry, as previously described (8). Briefly, 100 μl of PSCOOH particle suspension was washed and diluted 4-fold in ultrapure water. A 5-fold excess of methoxy-PEG-amine was added to the particle suspension and mixed to dissolve. N-hydroxysulfosuccinimide sodium salt (sulfo-NHS; Sigma-Aldrich, St. Louis, MO) was added followed by 200 mM borate buffer (pH 8.2) and 1-ethyl-3-(3-dimethylaminopropyl) carbodiimide (EDC; Invitrogen, Carlsbad, CA) at a final concentration of 10 mM. Particle suspensions were placed on a rotary incubator for 4 h at 25°C. Particles were washed and resuspended in ultrapure water to the original concentration. Aliquots for particle transport analysis were appropriately diluted in ultrapure water and stored at 4°C until use.

Particle hydrodynamic diameter, PDI, and ζ-potential were measured by dynamic light scattering and laser Doppler anemometry using a Zetasizer Nano ZS90 (Malvern Instruments, Malvern, UK) with a 90° scattering angle. Measurements were conducted at 25°C with particles suspended in phosphate buffered 10 mM NaCl, pH 7.4. We recently measured the surface density of PEG on PSPEG particles prepared via this protocol to be ~0.09 PEG/nm^2 using a nuclear magnetic resonance (NMR) method (8). The ability of MIP to resist mucoadhesion was

determined by comparing the amount protein adsorbed on the surfaces of MAP and MIP following their incubation in mucin solution using BCA assay (9).

Multiple particle tracking analysis

Nanoparticle transport in sputum was measured by multiple particle tracking (MPT). Aliquots (~30 μl) from the relatively solid or uniform portions of sputum were taken out of the sputum sample using a Wiretrol (Drummond Scientific Company, Broomall, PA) and placed in custom microslide chambers. Diluted nanoparticle suspensions were added to the sputum at a final dilution of ~3% v/v. A 0.5 μl aliquot of green fluorescent MAP plus 0.5 μl of red fluorescent MIP with each particle size (100, 300, and 500 nm) were added to each chamber. The samples were gently stirred and the chambers were sealed with a coverslip to prevent sample dehydration and equilibrated for 30 minutes before imaging. The chambers were imaged at room temperature using an inverted epifluorescence microscope (Axio Observer; Zeiss, Germany) on a vibration table with a 100x/1.46 NA oil-immersion objective. Movies were recorded for 20 s at a temporal resolution of 67 ms using an EM-CCD camera (Evolve 512; Photometrics, Tuscan, AZ).

Movies were analyzed with a custom automated particle tracking software in MATLAB (Mathworks; Natick, MA) to extract the *x* and *y* positions of particle centroids over time (10, 11). At least 100 particles of each size and type were tracked for a minimum of 50 frames. The time-averaged mean squared displacement (MSD) as a function of time scale, τ, was calculated for each particle trajectory as $\langle \Delta r^2(\tau) \rangle = \langle [x(t+\tau) - x(t)]^2 \rangle + \langle [y(t+\tau) - y(t)]^2 \rangle$. Sputum samples were assumed to be locally isotropic (although not homogenous), thus the 2D MSD measured can be extrapolated to 3D MSD (12). Median MSD values were reported for each sample instead of the ensemble average due to the inherent heterogeneity, and non-normal distribution of muco-inert nanoparticle (MIP) diffusion in COPD sputum (13). Previously we showed that the estimated static error is much smaller than the particle displacements, therefore

static error is not expected to significantly impact the calculated MSD (14). Additionally, we previously found that the effect of static and dynamic error in MPT experiments was minimized for MSD measured at $\tau = 1$ s (MSD_{1s}). Thus, $\log_{10}$(median $MSD_{\tau=1s}$) was used as our primary measurement readout (10, 11, 14). Microscope resolution was determined by analyzing MSD on stuck particles in glue between two coverslips, which was deemed to be less than Log(MSD) of -3. Pore size measurements were determined by obstruction-scaling model based on MSD values, which is previously described (2).

Measurement of total solids, mucin, and DNA content

The total solids content of sputum was determined by freeze-drying. Sputum sample aliquots of known mass were frozen in liquid N_2 and lyophilized (Labconco, Kansas City, MO) for at least 12 h to remove water from the samples. The sputum solid content is calculated as the ratio of dry mass to wet mass.

Mucin concentration was determined based on the reaction of 2-cyanoacetamide (Sigma-Aldrich) with O-linked glycoproteins, as previously described (15, 16). Sputum aliquots were diluted 20-fold and homogenized by vortexing for at least 15 min. Then, 50 μl of the suspension was reacted with 60 μl of an alkaline solution of 2-cyanoacetamide (200 μl of 0.6 M 2-cyanoacetamide mixed with 1 ml of 0.15 M NaOH) at 100ºC for 30 min. After incubation, 0.5 ml of 0.6 M borate buffer, pH 8.0, was added and the fluorescence intensity was measured at excitation and emission wavelengths of 336 and 383 nm, respectively. Sputum mucin concentrations were calculated with reference to a standard curve generated using known concentrations of mucin from bovine submaxillary gland (Sigma-Aldrich).

DNA concentration was measured using a fluorometric assay based on the reaction of diaminobenzoic acid (DABA; Sigma-Aldrich) with DNA, as previously described (15). Sputum aliquots were diluted 5-fold and homogenized by vortexing for at least 15 min. Next, 30 μl of this

suspension was mixed with 30 μl of 20% w/v DABA solution and incubated at 60°C for 1 h. One ml of 1.76 M HCl was then added to stop the reaction. The fluorescence was measured at excitation and emission wavelengths of 390 and 530 nm, respectively. Sputum DNA concentrations were calculated based on a standard curve generated using known concentrations of DNA from salmon testes (Sigma-Aldrich).

Statistical analysis

Statistical significance of paired observations were determined using Wilcoxon signed rank test. Comparisons between more than two groups were derived by one-way analysis of variance (ANOVA) or the non-parametric Kruskal-Wallis test. Correlations between different biophysical and pulmonary function measurements were analyzed by Spearman's rank-order correlation. Calculations were performed using GraphPad Prism software. All P values were two-sided and $P < 0.05$ was considered significant.

References

1. Couper D, LaVange LM, Han M, Barr RG, Bleecker E, Hoffman EA, Kanner R, Kleerup E, Martinez FJ, Woodruff PG, Rennard S. Design of the Subpopulations and Intermediate Outcomes in COPD Study (SPIROMICS). *Thorax* 2014; 69: 491-494.
2. Duncan GA, Jung J, Joseph A, Thaxton AL, West NE, Boyle MP, Hanes J, Suk JS. Microstructural alterations of sputum in cystic fibrosis lung disease. *JCI Insight* 2016; 1: e88198.
3. Bestall JC, Paul EA, Garrod R, Garnham R, Jones PW, Wedzicha JA. Usefulness of the Medical Research Council (MRC) dyspnoea scale as a measure of disability in patients with chronic obstructive pulmonary disease. *Thorax* 1999; 54: 581-586.
4. Celli BR, Cote CG, Marin JM, Casanova C, Montes de Oca M, Mendez RA, Pinto Plata V, Cabral HJ. The body-mass index, airflow obstruction, dyspnea, and exercise capacity index in chronic obstructive pulmonary disease. *The New England journal of medicine* 2004; 350: 1005-1012.
5. Jones PW, Quirk FH, Baveystock CM, Littlejohns P. A self-complete measure of health status for chronic airflow limitation. The St. George's Respiratory Questionnaire. *The American review of respiratory disease* 1992; 145: 1321-1327.
6. Ware J, Jr., Kosinski M, Keller SD. A 12-Item Short-Form Health Survey: construction of scales and preliminary tests of reliability and validity. *Medical care* 1996; 34: 220-233.
7. Jones PW, Harding G, Berry P, Wiklund I, Chen WH, Kline Leidy N. Development and first validation of the COPD Assessment Test. *The European respiratory journal* 2009; 34: 648-654.
8. Nance EA, Woodworth GF, Sailor KA, Shih TY, Xu Q, Swaminathan G, Xiang D, Eberhart C, Hanes J. A dense poly(ethylene glycol) coating improves penetration of large polymeric nanoparticles within brain tissue. *Science translational medicine* 2012; 4: 149ra119.
9. Mastorakos P, da Silva AL, Chisholm J, Song E, Choi WK, Boyle MP, Morales MM, Hanes J, Suk JS. Highly compacted biodegradable DNA nanoparticles capable of overcoming the mucus barrier for inhaled lung gene therapy. *Proceedings of the National Academy of Sciences of the United States of America* 2015; 112: 8720-8725.
10. Schuster BS, Ensign LM, Allan DB, Suk JS, Hanes J. Particle tracking in drug and gene delivery research: State-of-the-art applications and methods. *Advanced drug delivery reviews* 2015.
11. Schuster BS, Kim AJ, Kays JC, Kanzawa MM, Guggino WB, Boyle MP, Rowe SM, Muzyczka N, Suk JS, Hanes J. Overcoming the cystic fibrosis sputum barrier to leading adeno-associated virus gene therapy vectors. *Molecular therapy : the journal of the American Society of Gene Therapy* 2014; 22: 1484-1493.
12. Suh J, Dawson M, Hanes J. Real-time multiple-particle tracking: applications to drug and gene delivery. *Adv Drug Deliv Rev* 2005; 57: 63-78.
13. Feinstein AR. Principles of Medical Statistics. Chapman and Hall/CRC; 2001.
14. Kim AJ, Boylan NJ, Suk JS, Hwangbo M, Yu T, Schuster BS, Cebotaru L, Lesniak WG, Oh JS, Adstamongkonkul P, Choi AY, Kannan RM, Hanes J. Use of single-site-functionalized PEG dendrons to prepare gene vectors that penetrate human mucus barriers. *Angew Chem Int Ed Engl* 2013; 52: 3985-3988.
15. Sanders NN, De Smedt SC, Van Rompaey E, Simoens P, De Baets F, Demeester J. Cystic fibrosis sputum: a barrier to the transport of nanospheres. *American journal of respiratory and critical care medicine* 2000; 162: 1905-1911.
16. Crowther RS, Wetmore RF. Fluorometric assay of O-linked glycoproteins by reaction with 2-cyanoacetamide. *Analytical biochemistry* 1987; 163: 170-174.

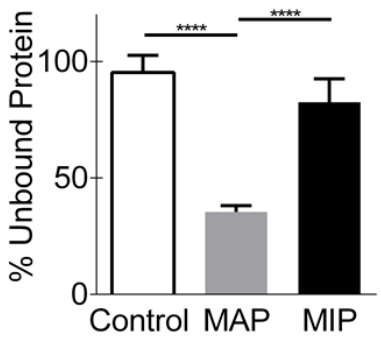

Supplemental Figure S1. Adsorption of mucin on the surfaces of 100 nm MAP and MIP. Unbound protein following a 30-minute incubation of nanoparticles (0.001 mg/mL), including MAP and MIP, in a mucin solution (0.01 mg/mL) was quantified. Data represent the mean ± SEM and are labeled as significant (N = 3, ****$p < 0.0001$, one-way ANOVA).

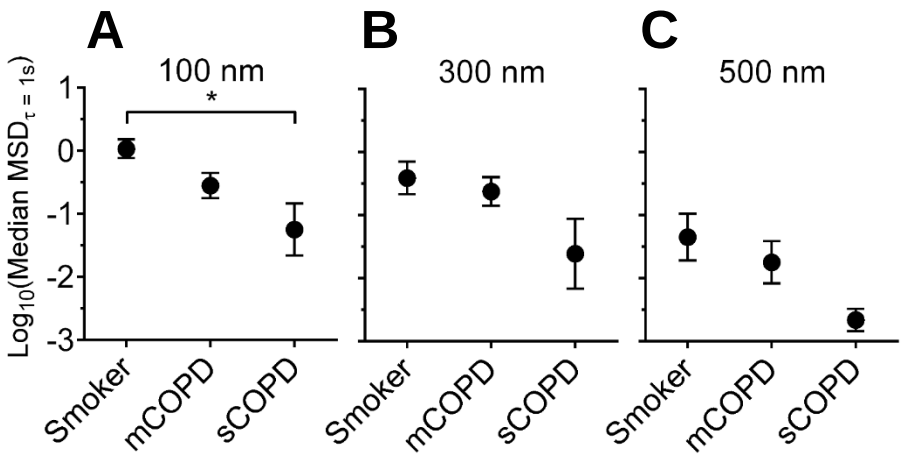

Supplemental Figure S2. Logarithmic median MSD of MIP probes in spontaneously expectorated sputum from non-COPD smokers and COPD patients stratified for COPD severity based on spirometric pulmonary function measurements. Microstructural analysis of different patient groups by different MIP particle diameters of (**A**) 100 nm, (**B**) 300 nm and (**C**) 500 nm. All data represent N ≥ 3 sputum samples. Data represented as mean ± SEM. Data labeled as statistically significant (*$p < 0.05$, Kruskal-Wallis test).

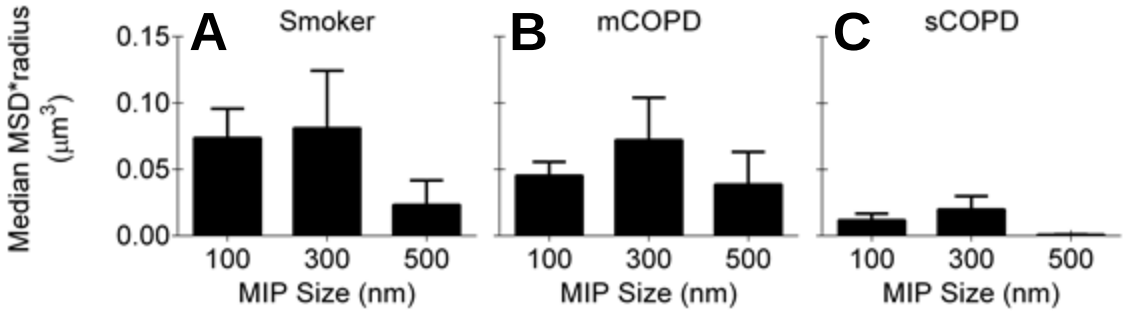

Supplemental Figure S3. Comparison between size-corrected MSD in spontaneously expectorated sputum from non-COPD smokers and COPD patients stratified for COPD severity based on spirometric pulmonary function measurements. Quantification of Median MSD multiplied by particle radius in (**A**) Smoker, (**B**) mCOPD and (**C**) sCOPD groups. MIP

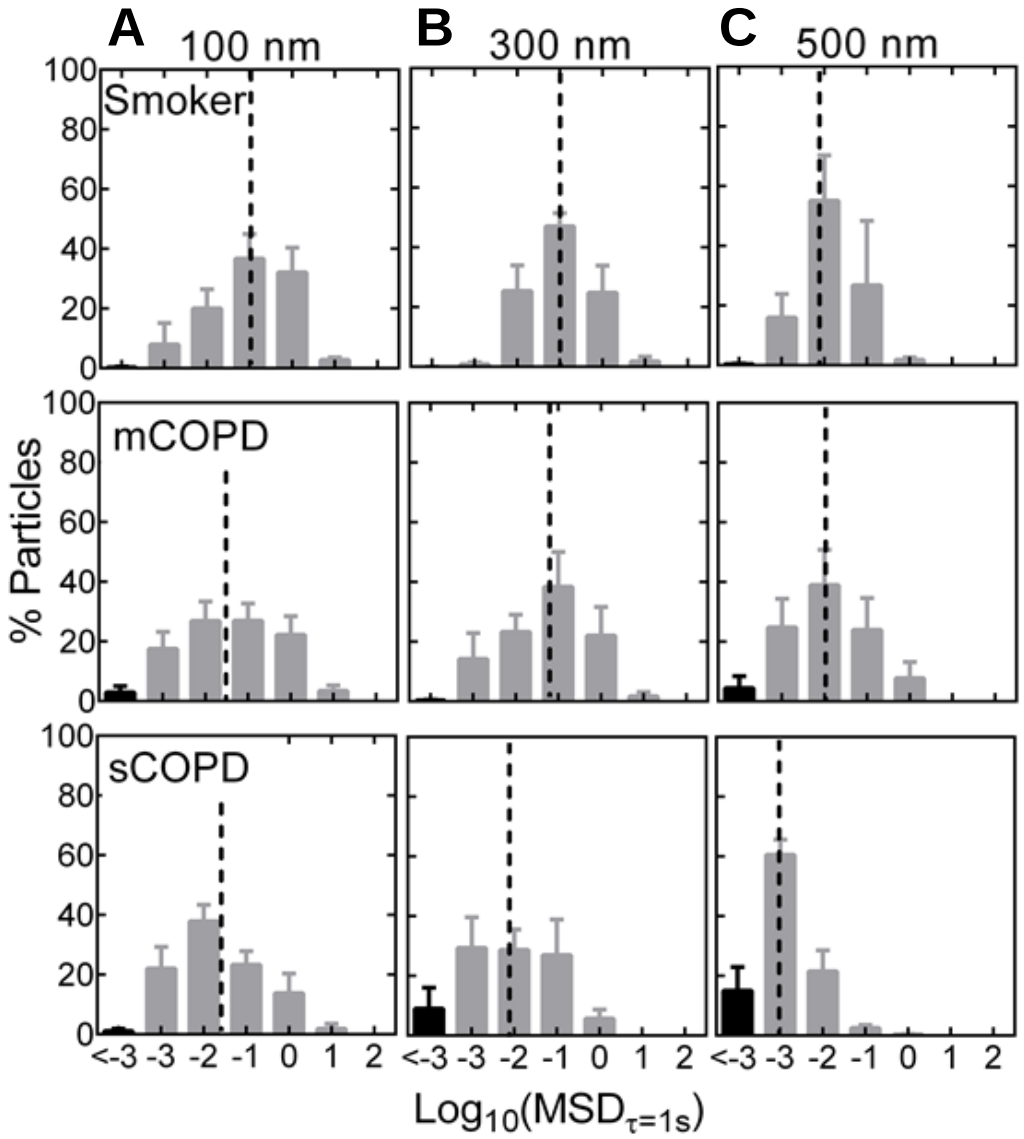

Supplemental Figure S4. Diffusion of differently sized MAP in spontaneously expectorated sputum from non-COPD smokers and COPD patients stratified for COPD severity based on spirometric pulmonary function measurements. Subjects are categorized into one of the three groups: non-COPD cigarette smokers (Smoker), mild COPD (mCOPD), and severe COPD (sCOPD). Distribution of the $\log_{10}(MSD_{\tau=1s})$ of individual MAP with particle sizes of: **(A)** 100 nm, **(B)** 300 nm, and **(C)** 500 nm. Data represents N ≥ 5 sputum samples with at least 500 particles tracked. The median of the distribution of $\log_{10}(MSD_{\tau=1s})$ for each set is indicated by the dashed line. Black bar represents values below tracking resolution.

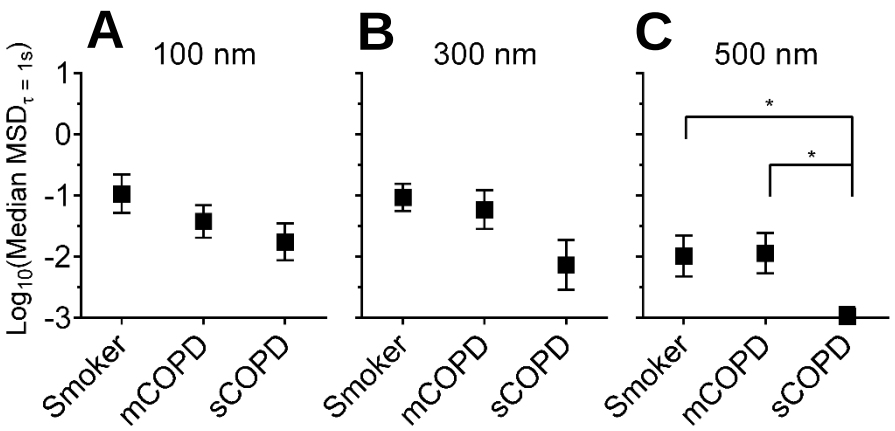

Supplemental Figure S5. Logarithmic median MSD of MAP probes in spontaneously expectorated sputum from non-COPD smokers and COPD patients stratified for COPD severity based on spirometric pulmonary function measurements. Quantification of $\log_{10}$(median $MSD_{\tau=1s}$) in different patient groups by MAP probes of (**A**) 100 nm, (**B**) 300 nm and (**C**) 500 nm particle diameters. All data represent N ≥ 3 sputum samples. Data represented as mean ± SEM. Data labeled as statistically significant (*p < 0.05, Kruskal-Wallis test).

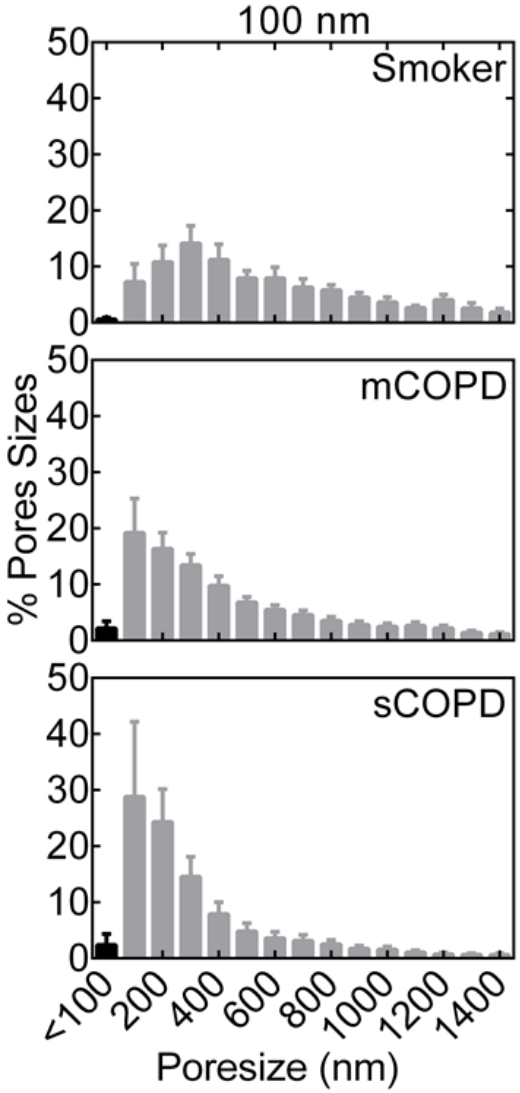

Supplemental Figure S6. Distribution of pore sizes derived from MSD of 100 nm of MIP in spontaneously expectorated sputum from non-COPD smoker and COPD patients stratified for COPD severity based on spirometric pulmonary function measurement. Mesh pore sizes of COPD sputum were calculated by MSD values and the obstruction-scaling model as previously described [1]. Data represents N ≥ 5 sputum samples with at least 500 particles tracked. Black bar represents values based on MSD below tracking resolution.

References

1. Duncan GA, Jung J, Joseph A, Thaxton AL, West NE, Boyle MP, Hanes J, Suk JS. Microstructural alterations of sputum in cystic fibrosis lung disease. *JCI insight* 2016: 1(18): e88198.